

PHYSICAL REVIEW D

PARTICLES AND FIELDS

THIRD SERIES, VOLUME 42, NUMBER 8

15 OCTOBER 1990

Thermal noise in mechanical experiments

Peter R. Saulson*

*Joint Institute for Laboratory Astrophysics, National Institute of Standards and Technology,
and University of Colorado, Boulder, Colorado 80309-0440*

(Received 8 June 1990)

The fluctuation-dissipation theorem is applied to the case of low-dissipation mechanical oscillators, whose losses are dominated by processes occurring inside the material of which the oscillators are made. In the common case of losses described by a complex spring constant with a constant imaginary part, the thermal noise displacement power spectrum is steeper by one power of ω than is predicted by a velocity-damping model. I construct models for the thermal noise spectra of systems with more than one mode of vibration, and evaluate a model of a specific design of pendulum suspension for the test masses in a gravitational-wave interferometer.

I. INTRODUCTION

Thermal noise is one of the fundamental limits to the precision of mechanical measurements. Its importance in high-sensitivity galvanometers is well studied.¹ It is also one of the dominant noise sources in resonant-mass detectors of gravitational waves and a major reason that such detectors operate at cryogenic temperatures.² In both of these instruments, what is observed is that the thermal noise excites the mechanical resonance with a root-mean-square level that corresponds to an energy of $k_B T$.

In many experiments, it is the thermal noise far from the resonant frequency that is most important. In laser interferometer gravitational-wave detectors, for example, resonant mechanical systems are employed, but mainly in the role of vibration isolators, with the resonant frequencies lying below the signal band.³ Thermal noise motion of the test masses in the nearly free regime above the resonances is expected to be an important noise source, and thermal noise in the signal band from high-frequency internal resonances in the test masses may also be important. Other gravitational experiments employ delicate torsion balances. These are typically used in a mode where the signal frequency is well below the fundamental resonance.⁴ Thermal noise sets a significant noise floor in these measurements as well.

Models of thermal noise almost invariably assume that the dissipative force is proportional to velocity. (Notable exceptions are the work of Speake and of Chan and Paik.⁵) However, in the low-loss oscillators typically used in sensitive gravitational experiments, the dependence of the dissipation on frequency seldom obeys this expected

behavior. Calculations of thermal noise based on velocity-damping models can be seriously in error. In this paper I will discuss more realistic models of mechanical oscillators with small dissipation.

II. BROWNIAN MOTION

Brownian motion of a particle of mass m , subject to a frictional force of the form $F_{\text{friction}} = -fv$, is described by the Langevin equation⁶

$$m\ddot{x} + f\dot{x} = F_{\text{th}} \quad (1)$$

where F_{th} is a random force with a white spectral density:

$$F_{\text{th}}^2(\omega) = 4k_B T f \quad (2)$$

(Throughout this paper, I will use angular frequencies, with dimensions of rad/s, but will give power spectral densities referred to the customary 1-Hz bandwidth.) As is well known, the fluctuating force F_{th} comes about because of the randomness of the individual impacts from the molecules that make up the medium responsible for the deterministic force F_{friction} .

A damped harmonic oscillator [like the one shown in Fig. 1(a)] can be described by adding a term representing a Hooke's law restoring force $F_{\text{spring}} = -kx$, giving

$$m\ddot{x} + f\dot{x} + kx = F_{\text{th}} \quad (3)$$

This equation of motion is easy to solve in the frequency domain, by replacing $x(t)$ with $x(\omega)e^{i\omega t}$. Then the power spectral density of the position of the mass can be shown to be

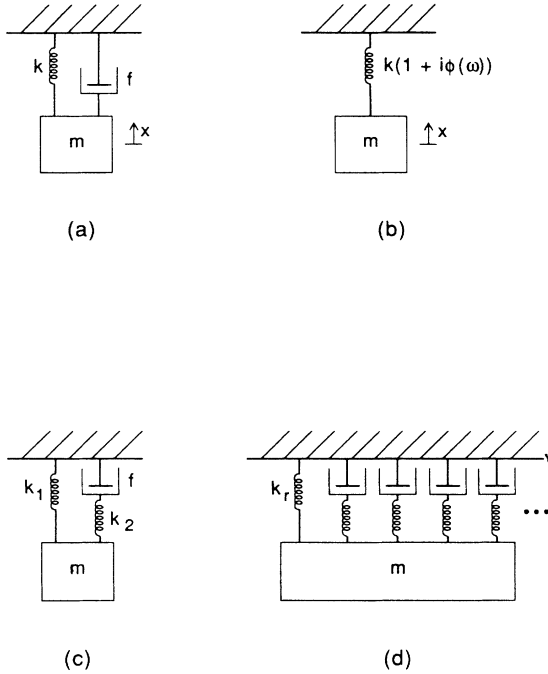


FIG. 1. (a) Schematic diagram of a mechanical oscillator consisting of a mass m , a spring of real spring constant k , and a dashpot with velocity coefficient f . (b) An oscillator consisting of a mass m and a spring with complex spring constant $k[1+i\phi(\omega)]$. (c) Schematic diagram of a standard anelastic solid. An ideal spring is connected in parallel with a spring-dashpot combination called a Maxwell unit. (d) Schematic model of an oscillator with an arbitrary frequency-dependent spring constant, constructed from a single ideal spring and many Maxwell units.

$$x^2(\omega) = \frac{4k_B T f}{(k - m\omega^2)^2 + f^2\omega^2} \quad (4)$$

A graph of this power spectrum (for a representative set of the parameters k , m , and f) is shown in Fig. 2. If f is small, then the response of the particle is sharply peaked near $\omega_0 = \sqrt{k/m}$. It is customary to denote the sharpness of the resonance by $Q \equiv \omega_0/\Delta\omega$, where $\Delta\omega$ is the full width measured at the half-power points. For the velocity-damped harmonic oscillator, $Q = m\omega_0/f$.

Predictions for the thermal noise in many delicate mechanical experiments have been made based on such models. In the next section I will set up a framework for more realistic models.

III. FLUCTUATION-DISSIPATION THEOREM

The fluctuations analogous to Brownian motion in any system with dissipation may be found using the fluctuation-dissipation theorem of Callen *et al.*⁷ The spectral density of the thermal driving force is given by

$$F_{th}^2(\omega) = 4k_B T R(\omega), \quad (5)$$

where $R(\omega)$ is the mechanical resistance, the real part of the impedance $Z \equiv F/v$ at the mass. Equivalently, the power spectrum of the motion of the mass is given by

$$x^2(\omega) = \frac{4k_B T \sigma(\omega)}{\omega^2}, \quad (6)$$

with $\sigma(\omega)$ denoting the mechanical conductance, the real part of the admittance $Y(\omega) \equiv Z^{-1}(\omega)$.

For the simple oscillator described above, the impedance is

$$Z = f + i\omega m + \frac{k}{i\omega}. \quad (7)$$

The admittance is

$$Y = \frac{\omega^2 f + i(\omega k - m\omega^3)}{(k - m\omega^2)^2 + \omega^2 f^2}. \quad (8)$$

Substituting the real part of Eq. (8) into Eq. (6), we obtain the same result for the displacement power spectrum as we did using the Langevin equation directly.

IV. EXTERNAL VELOCITY DAMPING

There are several common sources of damping that give forces proportional to velocity. The classic example is the viscous drag on a Brownian particle suspended in a liquid. A few high-precision experiments operate at high enough pressure so that the drag from the residual gas is in the viscous regime.⁸

Most gravitational experiments are performed at low pressures (around 10^{-6} Torr or lower). When the mean free path is large compared to a characteristic dimension of the test object, a description in terms of viscosity is no longer applicable. Instead, one must calculate the sum of the momentum transfer between the test object and each of the gas molecules that collide with it. It can be shown that the oscillator Q can be estimated as⁹⁻¹²

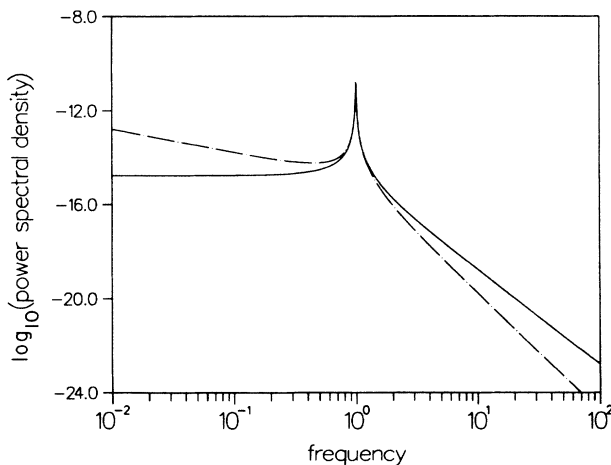


FIG. 2. Thermal noise power spectra for two mechanical oscillators, each with $m = 1$ g, resonant frequency $\omega_0 = 1$ s⁻¹, and $Q = 100$. The solid line shows the spectrum for an oscillator with damping proportional to velocity. The dash-dotted line shows the spectrum for an oscillator with internal damping characterized by constant $\phi(\omega)$. The units of the power spectral density are cm²/Hz and of the frequency axis are s⁻¹.

$$Q_{\text{gas}} = Ch \frac{\rho \omega_0}{n \sqrt{m_{\text{mol}} k_B T}} . \quad (9)$$

Here ρ is the density of the oscillator mass, n is the number density of gas molecules, each of which has mass m_{mol} , h is a characteristic dimension of the oscillator, and C is a dimensionless constant of order unity that depends on the shape of the oscillator.

For a 1-Hz pendulum of mass 10 kg, operating at pressures below 10^{-6} Torr, values of Q_{gas} in excess of 10^9 should be readily attainable. This means that gas damping can be made negligible compared to the internal damping mechanisms described in Sec. V. Torsion balances, on the other hand, typically have much smaller values of h and ω_0 , and so gas damping is often an important source of dissipation for them.^{4,10}

Eddy currents in moving conductors also give a damping force that is proportional to velocity.¹⁰ Good magnetic shielding, and use of nonconductors wherever possible, can reduce this to small levels.

V. INTERNAL DAMPING

Internal damping in materials has been found¹³ to obey an extension of Hooke's law, which can be approximated by

$$F = -k[1 + i\phi(\omega)]x . \quad (10)$$

If the force F is sinusoidal, the response x of the spring will lag the force by the angle $\phi(\omega)$. The time average of the product $F\dot{x}$ is proportional to ϕ (as long as $\phi \ll 1$). A fraction $2\pi\phi$ of the energy stored in the oscillatory motion is being dissipated during each cycle. Thus a complex spring constant is inevitably associated with damping. In turn, the fluctuation-dissipation theorem guarantees that damping generates mechanical noise.

It is instructive to study a simple mathematical model of an oscillator, substituting a general spring "constant" of the form of Eq. (10) for the velocity-damping term [see Fig. 1(b)]. The equation of motion becomes

$$m\ddot{x} = -k(1 + i\phi)(x - x_g) + F . \quad (11)$$

The vibration transfer function is

$$\frac{x}{x_g} = \frac{\omega_0^2(1 + i\phi)}{\omega_0^2 - \omega^2 + i\phi\omega_0^2} . \quad (12)$$

By comparison with Eq. (4), it is easy to see that an oscillator of this sort has a quality factor given by

$$Q = \frac{1}{\phi(\omega_0)} . \quad (13)$$

The mechanical impedance at the mass is

$$Z = i\omega m + \frac{k}{i\omega} + \frac{k\phi}{\omega} , \quad (14)$$

and so the thermal noise force spectral density is proportional to the quantity $k\phi(\omega)/\omega$ in place of the velocity coefficient f . The admittance is

$$Y = \frac{\omega k \phi + i(\omega k - m\omega^3)}{(k - m\omega^2)^2 + k^2\phi^2} . \quad (15)$$

The thermal noise power spectral density is given, according to the fluctuation-dissipation theorem, by

$$x^2(\omega) = \frac{4k_B T k \phi(\omega)}{\omega[(k - m\omega^2)^2 + k^2\phi^2]} . \quad (16)$$

VI. FORMS OF INTERNAL DAMPING

By far the most common functional form for $\phi(\omega)$ in materials of many kinds is ϕ approximately constant over a large band of frequencies.¹⁴ [The lag function $\phi(\omega)$ can be any odd function of frequency.¹⁵ Constant $\phi(\omega)$ is consistent with this condition as long as ϕ does not remain constant all the way to zero frequency.] In spite of the ubiquity of constant $\phi(\omega)$, there does not seem to be a simple model that gives a general explanation of the phenomenon. In some cases, a frequency-independent ϕ has been attributed to friction from dislocations.¹⁶

Sometimes, the damping exhibits a broad maximum at a characteristic frequency τ^{-1} . This is the classic phenomenon named "anelasticity" by Zener.¹⁷ Such behavior is caused by the functional dependence of some internal degree of freedom of the system upon the stress. For oscillatory stresses applied near τ^{-1} , the response of the material can lag substantially because of the finite time it takes for the internal degree of freedom (and consequently the strain of the material) to come to equilibrium.

A simple model, called the standard anelastic solid, can be used to represent the relaxation process described in the previous paragraph. One way to represent this model is by an arrangement of two springs and a dashpot, as shown in Fig. 1(c). The spring constant k_1 is called the "relaxed spring constant," and the sum $k_1 + k_2$ is called the "unrelaxed spring constant." (If the losses are small, then k_2 is much smaller than k_1 .) Zener showed that this model predicts that the loss angle ϕ depends on frequency with the characteristic form

$$\phi = \Delta \frac{\omega\tau}{1 + \omega^2\tau^2} , \quad (17)$$

as long as there are no other mechanisms with nearby relaxation times and $\phi \ll 1$. $\Delta \equiv k_2/k_1$ is called the "relaxation strength," while $\tau \equiv f/k_2$ is the "relaxation time."

VII. EQUIPARTITION THEOREM

The power spectrum of thermal noise will not in general have the functional form given in Eq. (4) for the case of velocity damping. For example, an oscillator with losses characterized by constant $\phi(\omega)$ has thermal noise whose power spectral density declines more rapidly with frequency (by one power of ω) than an oscillator subject to velocity damping (see the graph in Fig. 2). This means that if one had erroneously assumed velocity damping in a system with constant internal damping, one would have overestimated the thermal noise density for frequencies above the resonant frequency, but would have underes-

timated the noise in the region below the resonance. Relaxation damping, such as that described by the standard anelastic solid, also gives more noise at frequencies below $\omega_r \equiv 1/\tau$ than at higher frequencies.

The integral of Eq. (4) over all frequencies gives a mean-square displacement $\bar{x}_{\text{th}}^2 = k_B T/k$. This is, of course, consistent with the equipartition theorem, which states that each quadratic term in the energy has a mean value of $\frac{1}{2}k_B T$. Contrast the case of Eq. (16) for the case of $\phi(\omega)$ a constant. Here the integral diverges at $\omega=0$.

It is instructive to explore the relation between the equipartition theorem and thermal noise power spectra in general. First, it is important to point out that a spring constant of the form given in Eq. (10) is usually an excellent approximation, but it cannot be exact. For the standard anelastic solid of Fig. 1(c), a direct calculation gives a spring constant of

$$F = k_1 x \left[1 + \frac{\Delta \omega^2 \tau^2}{1 + \omega^2 \tau^2} + i \Delta \frac{\omega \tau}{1 + \omega^2 \tau^2} \right]. \quad (18)$$

Note the additional frequency-dependent real term. For the common case of small Δ , this term is usually negligible compared to the constant term. The heuristic interpretation is that at high frequencies the effective spring constant is the unrelaxed spring constant $k_1 + k_2$, because the dashpot appears rigid. At low frequencies, the dashpot is free to move, and so the effective spring constant is just the relaxed spring constant k_1 .

This is a special case of a theorem usually attributed to Bode,¹⁸ stating that there is a unique relationship between the phase of a network characteristic (such as a transfer function, impedance, admittance, or spring constant) and the functional form of its magnitude, as long as it has no poles or zeros in the right half of the complex plane. For example, such a function with magnitude proportional to ω^n has constant phase of $n\pi/2$. Applied to a spring with constant phase ϕ , the theorem requires that the magnitude is proportional to $\omega^{2\phi/\pi}$. For a low-loss spring, this is an extremely weak dependence on frequency, which is why it is usually neglected.

In order to understand mean-square thermal noise displacements, it is important to keep in mind the weak variation of a spring constant with frequency. Again, let us consider first the standard anelastic solid. Direct integration of the thermal noise power spectrum gives the result $\bar{x}_{\text{th}}^2 = k_B T/k_1$. This is also the result expected from the equipartition theorem, since the displacement of the mass is equal to the extension of the energy storage element k_1 , the relaxed spring constant.

A similar explanation can be given for other forms of the frequency-dependent spring constant. It is always possible to represent an arbitrary lossy spring with a model such as the one shown in Fig. 1(d). Here the single spring-dashpot element of the standard anelastic solid is replaced by a spectrum of such elements, whose spring constants and relaxation times are adjusted to give the observed frequency dependence. (Various methods to construct such a model are discussed by Nowick and Berry.¹³) The spectrum contains a longest relaxation time τ_{max} . At frequencies below $1/\tau_{\text{max}}$, the spring behaves

like the ideal spring k_r . [The requirement that there exist a longest relaxation time is a restatement of the realizability condition that $\phi(\omega)$ be an odd function of ω .] The equipartition theorem then states that $\bar{x}_{\text{th}}^2 = k_B T/k_r$.

A real experimental measurement of the mean-square displacement cannot integrate all the way to $\omega=0$, but only down to a frequency $\omega \approx 1/\tau_{\text{int}}$, where τ_{int} is the duration of the measurement. Thus, if $\tau_{\text{max}} > \tau_{\text{int}}$, one should not expect the equipartition theorem to hold exactly. Instead, we expect the approximate relation $\bar{x}_{\text{th},\tau}^2 \approx k_B T/k(1/\tau_{\text{int}})$, where $\bar{x}_{\text{th},\tau}^2$ is the mean-square displacement as measured in the finite integration time, and $k(1/\tau_{\text{int}})$ is the magnitude of the spring constant at a frequency $\omega = 1/\tau_{\text{int}}$. This can be interpreted in light of a model of the form shown in Fig. 1(d). For measurements extending only to τ_{int} , all of the spring-dashpot elements that have $\tau > \tau_{\text{int}}$ behave as if their spring constants were added to k_r . Thus the effective relaxed spring constant is approximately $k(1/\tau_{\text{int}})$.

The contribution of the formally divergent part of the integral (for ϕ constant) will be quite small in most experiments. This is because in a lightly damped oscillator, most of the power is in the resonant peak itself. In the case of velocity damping, only roughly $1/Q$ of the mean-square displacement comes from frequencies below the resonance. For damping with constant ϕ , the highest octave below the resonance thus contains approximately the fraction ϕ of the total thermal noise power. Each octave lower in frequency contains the same power, since the power spectral density is proportional to $1/\omega$. In particular, to obtain a power comparable to that in the resonant peak, this behavior must extend down in frequency for ϕ^{-1} octaves below the resonance. At such a low frequency, the magnitude of the spring constant has declined by about a factor of 2 below its unrelaxed value k_u . Thus the integral of the power spectrum down to such a frequency is consistent with the prediction $\bar{x}_{\text{th}}^2 = k_B T/(k_u/2)$.

A numerical example will help to put this issue in perspective. Consider a 1-Hz oscillator that has damping characterized by frequency independent $\phi = 10^{-3}$. In order to measure a mean-square displacement twice the velocity-damping prediction, it would be necessary to use an integration time of roughly 10^{300} s. Clearly, the low-frequency divergence of Eq. (16) is of more formal than practical concern.

VIII. THERMOELASTIC DAMPING

As an example of anelasticity, consider the mechanism known as thermoelastic damping. This can be an important source of losses for thin samples in flexure. The internal degree of freedom involved is the temperature, which couples to the strain because materials have nonzero coefficients of thermal expansion. As a wire is flexed, one side heats and the other cools. Heat flows to attempt to restore equilibrium, causing the restoring force from the wire to relax from its initial value to a smaller equilibrium value.

The theory of this mechanism was given by Zener.¹⁹

He showed that this mechanism is well described by a model of the form described above, with the parameters

$$\Delta = \frac{E\alpha^2 T}{c}, \quad (19)$$

and

$$f_0 = \frac{1}{2\pi\tau} = 2.16 \frac{D}{d^2}. \quad (20)$$

Here E is the (unrelaxed) Young's modulus of the material, α is the linear coefficient of thermal expansion, and c is the specific heat per unit volume. In Eq. (20), d is the diameter of the wire, and the thermal diffusion coefficient D is given by $D = \kappa/c$, where κ is the thermal conductivity. Note that this damping mechanism depends only on the sort of properties of a material that are tabulated in handbooks, and not on details of its structure or composition.

Zener gave the solution not only for wires, but also for ribbons of rectangular cross section. The sole difference is that the characteristic frequency is given by

$$f_0 = \frac{\pi}{2} \frac{D}{t^2}, \quad (21)$$

where t is the thickness of the ribbon. Thus, if the characteristic frequency is larger than the frequencies of interest, the thermoelastic damping effect can be reduced by flattening the suspension member. This occurs at the expense, of course, of introducing an anisotropy into the compliance of the suspension.

I have given prominent treatment to the thermoelastic relaxation mechanism because it sets a fundamental limit beyond which the losses cannot be reduced, given a choice of wire material and geometry. Note that thermoelastic relaxation is of no consequence for the longitudinal modes of wires (vertical modes of a pendulum), since the relevant length scale is not the thickness of the wire but the acoustic wavelength in the wire. (Note also that if the oscillator in question was a torsion pendulum, then thermoelastic damping cannot apply, since torsional motion involves only shear, nowhere expansion or contraction.)

Other relaxation mechanisms depend on much more obscure properties of a specimen. Nowick and Berry¹³ stress the use of experiments on anelastic behavior as a probe of the structure of solids.

IX. PENDULUM

The universal choice of a pendulum as the final suspension stage in gravitational-wave interferometers is based on the desire to minimize thermal noise. In a pendulum, the primary "spring" for horizontal motion is the gravitational field, with only a small amount of restoring force coming from flexure of the wire that supports the mass against gravity. The gravitational spring is free of loss,

and so the only mechanical loss is the fraction $2\pi\phi(\omega)$ per cycle of the mechanical energy stored in the flexing wire. That is, the relationship between the pendulum loss ϕ_p and the loss in the wire ϕ_w is given by

$$\phi_p = \phi_w \frac{E_{el}}{E_{grav} + E_{el}} \approx \phi_w \frac{E_{el}}{E_{grav}}, \quad (22)$$

where E_{el} and E_{grav} represent, respectively, the energy stored in the flexing wire and in the gravitational field.¹² Thus a pendulum can have much lower loss than the material of which it is made.

This calculation can be made more explicit by remembering that $E_{el}/E_{grav} = k_{el}/k_{grav}$. The gravitational spring constant is of course $k_{grav} = mg/l$ for a pendulum of length l . The elastic spring constant for a pendulum in which the mass is supported by n wires is $k_{el} = n\sqrt{TEI}/2l^2$, where T is the tension in each wire, E is the Young's modulus, and I is the moment of inertia of the wire cross section. Substituting into Eq. (22), we find that

$$\phi_p(\omega) = \phi_w(\omega) \frac{n\sqrt{TEI}}{2mgl}. \quad (23)$$

It is interesting to consider how the thermal noise in a pendulum scales with the mass. The explicit dependence, taking the high-frequency limit of Eq. (16), is $x^2(\omega) \propto m^{-1}$. But $\phi(\omega)$ [here $\phi_p(\omega)$] also depends on the suspended mass. In addition to the explicit dependence displayed in Eq. (23), remember that T is proportional to m , and if the wires are kept at a fixed fraction of their breaking stress, then $I \propto m^2$. Thus $\phi_p \propto m^{1/2}$, and so the thermal noise in a pendulum scales as²⁰

$$x_p^2(\omega) \propto m^{-1/2}. \quad (24)$$

A similar analysis shows that $x_p^2(\omega)$ also scales as $n^{-1/2}$.

X. MULTIMODE OSCILLATORS

The remainder of this paper is devoted to applications of the fluctuation-dissipation theorem to systems more complicated than a damped harmonic oscillator. A two-mode oscillator is perhaps the simplest of such systems. (Time-domain treatments of the problem have been given by Wang and Uhlenbeck⁶ and by Paik.⁹)

Consider the system shown schematically in Fig. 3. The equations of motion are

$$\begin{aligned} m_1 \ddot{x}_1 &= -k_1 x_1 - f_1 \dot{x}_1 - k_2(x_1 - x_2) - f_2(\dot{x}_1 - \dot{x}_2), \\ m_2 \ddot{x}_2 &= -k_2(x_2 - x_1) - f_2(\dot{x}_2 - \dot{x}_1) + F. \end{aligned} \quad (25)$$

It is useful to define the quantities $\omega_1^2 \equiv k_1/m_1$, $\omega_2^2 \equiv k_2/m_2$, $\beta_1 \equiv f_1/m_1$, $\beta_2 \equiv f_2/m_2$, and $\mu \equiv m_2/m_1$. Transforming the equations of motion into the frequency domain, we obtain the 2×2 matrix equation

$$\begin{bmatrix} \omega_1^2 + i\omega\beta_1 - \omega^2 + \mu(\omega_2^2 + i\omega\beta_2) & -\mu(\omega_2^2 + i\omega\beta_2) \\ -(\omega_2^2 + i\omega\beta_2) & \omega_2^2 + i\omega\beta_2 - \omega^2 \end{bmatrix} \begin{bmatrix} x_1 \\ x_2 \end{bmatrix} = \begin{bmatrix} 0 \\ F/m_2 \end{bmatrix}, \quad (26)$$

or

$$\mathbf{D}\mathbf{x}=\mathbf{F} . \tag{27}$$

Then it is easy to show that the impedance at the mass m_2 is

$$Z = \frac{m_2 \det(\mathbf{D})}{i\omega[\omega_1^2 + i\omega\beta_1 - \omega^2 + \mu(\omega_2^2 + i\omega\beta_2)]} , \tag{28}$$

where $\det(\mathbf{D})$ is the determinant of the matrix \mathbf{D} . Its real part is

$$R = \frac{m_2[\omega^6\beta_2 + \omega^4(\beta_1^2\beta_2 + \mu\beta_1\beta_2^2 - 2\beta_2\omega_1^2) + \omega^2(\beta_2\omega_1^4 + \mu\beta_1\omega_2^4)]}{\omega^6 + \omega^4(\beta_1^2 - 2\omega_1^2 + 2\mu(\beta_1\beta_2 - \omega_2^2) + \mu^2\beta_2^2) + \omega^2(\omega_1^4 + 2\mu\omega_1^2\omega_2^2 + \mu^2\omega_2^4)} . \tag{29}$$

This last expression, multiplied by $4k_B T$, gives the power spectral density of the thermal noise driving force applied to m_2 . In the limit of large frequency, the real part of the impedance approaches $m_2\beta_2 = f_2$, and so only the damping applied directly to m_2 matters. If that damping should be vanishingly small, the dominant term is $\mu^2 f_1 \omega_2^4 / \omega^4$.

For the case of $\mu=1$, $\omega_1=\omega_2=1$, $\beta_1=10^{-2}$, and $\beta_2=10^{-6}$, a graph of the thermal noise power spectrum is shown in Fig. 4. Note that both of the normal modes have a low Q , since both modes involve substantial motion of the more highly damped m_1 . Yet the thermal noise motion of m_2 in the limit of high frequency is determined only by the damping coefficient β_2 . This is in ac-

cord with the intuitive picture that the thermally driven fluctuations of m_1 can be thought of as an input to the lower oscillator that is filtered in the same way that the lower oscillator acts as a low-pass filter for vibration of any sort.

XI. MODES OF CONTINUOUS SYSTEMS

It is sometimes necessary to take account of the fact that real oscillators are distributed systems, not point masses and massless springs. A pendulum exhibits transverse vibrational modes in its wire(s), as well as longitudinal modes of its mass. This means that Eq. (16) applied to the fundamental mode of the pendulum will cease to apply at a high enough frequency, since eventually the thermal noise from another mode of higher resonant frequency will dominate.

The character of the solution is especially clear in the admittance formulation of the fluctuation-dissipation theorem. The expansion theorem²¹ states that the response of a system to an applied force is equal to the superposition of the responses of each of the normal modes of the system. Consider, for simplicity, a one-dimensional system with linear mass density $\rho(x)$. It has modes $\psi_n(x)$, which are normalized according to the relation

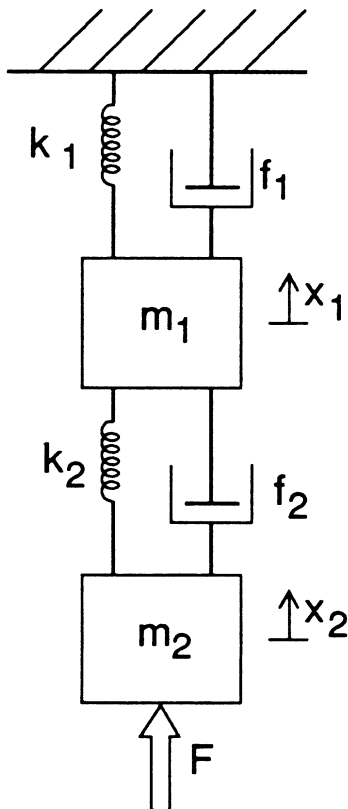


FIG. 3. Schematic diagram of a double oscillator. A force F may be applied to the second mass m_2 .

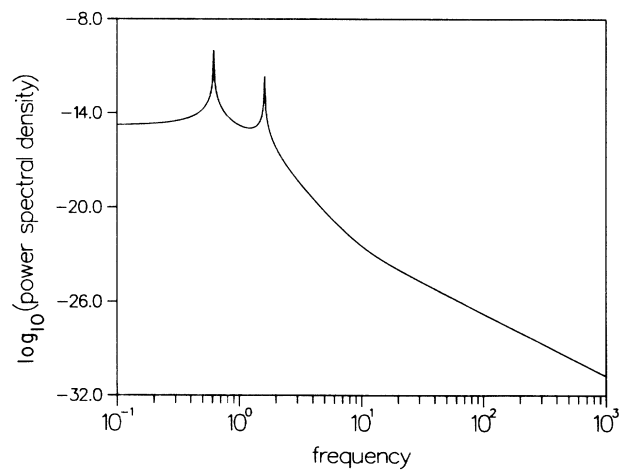


FIG. 4. Thermal noise power spectrum for a double oscillator. Each mass has $m = 1$ g. The other parameters of the oscillator are as given in the text.

$$\int_0^L \rho(x) \psi_m(x) \psi_n(x) dx = \delta_{mn} . \quad (30)$$

The normal-mode expansion of a particular displacement $y(x, t)$ is given by

$$y(x, t) = \sum_{n=1}^{\infty} \psi_n(x) q_n(t) , \quad (31)$$

where $q_n(t)$ is the generalized coordinate of mode n . Its equation of motion has the form

$$\ddot{q}_n(t) + \omega_n^2 q_n(t) = Q_n(t) . \quad (32)$$

Q_n is the n th generalized force, given by

$$Q_n(t) = \int_0^L f(x, t) \psi_n(x) dx , \quad (33)$$

with $f(x, t)$ being the force density applied to the system.

In particular, a force F applied at the end of the system $x = L$ is represented by generalized forces

$$Q_n = F \psi_n(L) . \quad (34)$$

Then we have, from Eq. (31) (after switching to the frequency domain and explicitly including a damping term),

$$q_n = \frac{F \psi_n(L)}{\omega_n^2 - \omega^2 + i \phi_n(\omega) \omega_n^2} . \quad (35)$$

Substituting into Eq. (31), we find

$$y(L) = \sum_{n=1}^{\infty} \frac{F \psi_n^2(L)}{\omega_n^2 - \omega^2 + i \phi_n(\omega) \omega_n^2} . \quad (36)$$

Thus the admittance, $Y = v/F$, is given by

$$Y = \sum_{n=1}^{\infty} \frac{i \omega \psi_n^2(L)}{\omega_n^2 - \omega^2 + i \phi_n(\omega) \omega_n^2} . \quad (37)$$

(This is just the superposition of the admittances of each of the normal modes.)

From the fluctuation-dissipation theorem [Eq. (16)], we can now find the thermal noise displacement at $x = L$:

$$x^2(\omega) = 4k_B T \sum_{n=1}^{\infty} \frac{\psi_n^2(L) \phi_n(\omega) \omega_n^2}{\omega [(\omega_n^2 - \omega^2)^2 + \phi_n^2(\omega) \omega_n^4]} . \quad (38)$$

This equation can be applied to the internal oscillations of the test mass in a gravitational-wave interferometer. The normal modes of a cylinder with an aspect ratio of order unity have a complicated mode shape.²² The problem can be treated as one dimensional, weighting each mode by a factor that represents the mean motion of the central part of the front surface of the cylinder along the optic axis. All of the modes with circumferential order greater than zero get zero weight (if the optical axis is aligned with the center of mass), while several of the gravest modes have weights of about unity. The factor $\psi_n^2(L) \approx 2/M$, where M is the mass of the test mass. By design the resonant frequencies ω_n are usually large compared to the frequency of interest, and so we can write

$$x^2(\omega) \approx \frac{8k_B T}{\omega} \sum_{n=1}^{\infty} \frac{\phi_n(\omega)}{M \omega_n^2} . \quad (39)$$

If, for example, $\phi(\omega)$ is constant, then the power spectral density is proportional to ω^{-1} .

It is interesting to consider again how the noise scales with the mass of the pendulum, as we did above for the fundamental mode. Here, in addition to the explicit factor of M^{-1} , the resonant frequencies have an implicit dependence on the mass. For a particular mode in a set of masses of the same aspect ratio, the quantity $\omega a/c$ is a constant, where a is the radius of the mass and c is the speed of sound. Since $M \propto a^3$ for any given material, then $\omega_n^2 \propto M^{-2/3}$. Thus we find $x^2(\omega) \propto M^{-1/3}$.

This argument assumes that the loss function $\phi_n(\omega)$ does not itself depend on the size of the mass. That assumption could be false if the dominant loss mechanism were some process involving only the surface of the mass.¹¹ In such a case, one might expect the loss to decrease as the mass increased, giving a stronger mass dependence to the thermal noise motion.

The transverse modes of a pendulum wire (“violin modes”) can also be modeled in this way. If we treat the pendulum as a wire of constant linear mass density ρ with a point mass M attached to the end at $x = L$, then the normalization equation, Eq. (30), becomes

$$\rho \int_0^L \psi_n^2(x) dx + M \psi_n^2(L) = 1 . \quad (40)$$

If we neglect the small stiffness of the wire, treating it as a perfectly flexible string under tension Mg , then the squared resonant frequencies are

$$\omega_n^2 = \frac{\pi^2 Mg}{\rho L^2} n^2 , \quad (41)$$

while the squared amplitudes are

$$\psi_n^2(L) = \frac{2\rho L}{\pi^2 M^2} \frac{1}{n^2} . \quad (42)$$

Thus the thermal noise power spectrum is

$$x^2(\omega) = \frac{8k_B T \rho^2 L^3}{\pi^4 M^3 g} \frac{1}{\omega} \sum_{n=1}^{\infty} \frac{\phi_n(\omega)}{n^4} . \quad (43)$$

Here, as for the fundamental mode of the pendulum, the loss $\phi_n(\omega)$ is only a small fraction of the loss of the wire material itself.

XII. RECOIL LOSSES

If a low-loss oscillator is suspended from a structure with low- Q resonances, then the loss at the resonant frequency may be substantially degraded. This effect may be analyzed in an approximate way by treating the system as a two-mode oscillator of the form shown in Fig. 3, with the resonant mode of the structure nearest in frequency to the mode of the sample playing the role of the upper oscillator. This is the same model discussed above, but here we are interested in what happens to the Q of the lightly damped resonance, instead of in the high-frequency behavior of the mechanical conductance. Thus, for the case of recoil damping as well as for a multimass oscillator, the thermal noise far from resonance may be substantially smaller than would be indicated by a naive interpretation of the damping of the resonance.

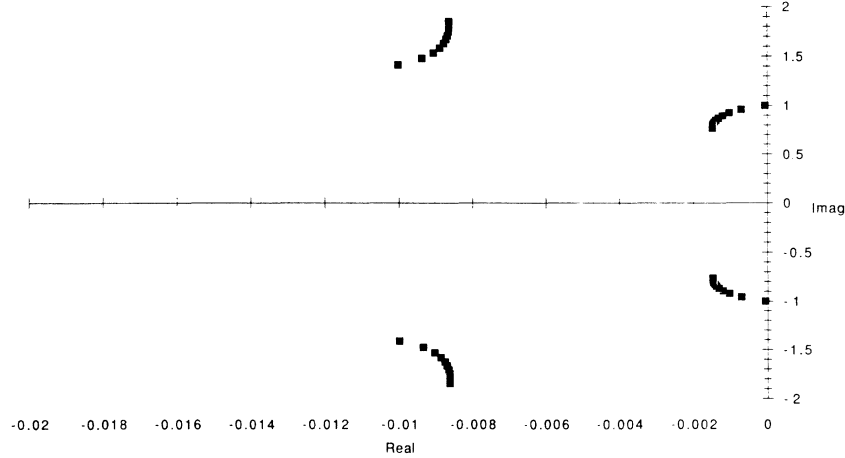


FIG. 5. Portion of the root locus for a double-oscillator model for recoil damping of a high- Q oscillator by resonances in its support structure. The high- Q oscillator has $\omega_2^2 = 1 \text{ s}^{-2}$ and $\beta_2 = 10^{-4}$. The structure is modeled as a mode with $\omega_1^2 = 2 \text{ s}^{-2}$ and $\beta_1 = 0.02$. The poles of the system are plotted for mass ratio $\mu = 0$ (infinite mass structure) to $\mu = 1$ (oscillator and structure of equal mass). Adjacent points are separated by $\Delta\mu = 0.1$. For clarity, the real and imaginary axes have been drawn to different scales.

The root locus method, a standard tool for the analysis of servomechanisms, is useful for the study of the dependence of the poles of any system on the values of parameters of the system.²³ The two-mode oscillator, analyzed with Laplace transform methods, is characterized by a transfer function

$$\frac{x_2}{F} = \frac{\omega_1^2 + \beta_1 s + s^2 + \mu(\omega_2^2 + \beta_2 s)}{(\omega_1^2 + \beta_1 s + s^2)(\omega_2^2 + \beta_2 s + s^2) + \mu s^2(\omega_2^2 + \beta_2 s)}. \quad (44)$$

The denominator has the same form as that of a servomechanism of loop transfer function

$$G(s) = \mu \frac{s^2(\omega_2^2 + \beta_2 s)}{(\omega_1^2 + \beta_1 s + s^2)(\omega_2^2 + \beta_2 s + s^2)}, \quad (45)$$

where the mass ratio $\mu \equiv m_2/m_1$ plays the role of an adjustable gain. We are interested primarily in how the Q of the lightly damped resonance ω_2 is changed by the recoil of the structure, as parametrized by μ . Figure 5 shows the locus of roots of the system as a function of μ , for one choice of the resonant frequencies and damping parameters.

It is possible to obtain a simple analytic expression for the recoil-damped Q of the oscillator, valid when the structure mass is much greater than the oscillator mass and when the structure has much more damping than the oscillator. The method sketched here makes use of the rules that govern the shape of the root locus in the vicinity of the zero-recoil ("open loop") poles.²³ The interesting features are the departure angle of the locus from the oscillator poles, and the relationship between the parameter μ and the distance traveled along the locus. The locus leaving one of the high- Q poles points almost directly toward the real axis, but has a fractional component of increasing real part of magnitude $\beta_1\omega_2/(\omega_1^2 - \omega_2^2)$. The distance traveled along the locus is given by $\mu\omega_2^3/2(\omega_1^2 - \omega_2^2)$. Combining these two results, one can show that

$$Q_{2,\text{recoil}}^{-1} \approx Q_2^{-1} + Q_1^{-1} \mu \frac{\omega_1 \omega_2^3}{(\omega_1^2 - \omega_2^2)^2}. \quad (46)$$

Thus recoil damping is most important when a support structure resonance is close in frequency to the sample resonance.

XIII. MODEL PENDULUM

In this section I estimate the thermal noise displacement power spectrum for a pendulum of a type that might be used as the suspension for the test masses in a gravitational-wave interferometer. A graph is shown in Fig. 6.

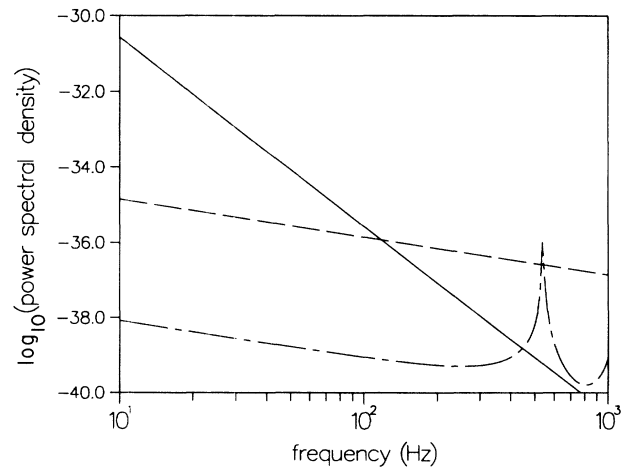


FIG. 6. Thermal noise power spectrum for the model pendulum described in the text. The solid line shows the thermal noise of the fundamental pendulum mode. The dash-dotted line shows the noise from the internal modes of the test mass. The third curve shows the noise from the modes of the pendulum wires. Note that for this graph the frequency axis is given in Hz.

A test mass in such an interferometer might have a mass of 10 kg, supported by four tungsten wires having a length $l = 30$ cm. Each wire has a diameter of 1.2×10^{-2} cm, so that it supports half of its breaking stress.²⁴ Measurements made by Kovalik and Saulson indicate that $\phi_w = 1 \times 10^{-3}$ (roughly independent of frequency) is an upper bound on the losses in tungsten wires.²⁵ The pendulum should then be characterized by $\phi_p = \phi_w (k_{el}/k_{grav}) = 5 \times 10^{-7}$. The resonant frequency is $\omega_0 \approx \sqrt{g/l} = 2\pi \times 0.9$ Hz. The thermal noise power spectral density, for frequencies large compared to the resonant frequency, is then $x^2(\omega) = (2.7 \times 10^{-26} \text{ cm}^2/\text{Hz})(2\pi \text{ s}^{-1}/\omega)^5$.

The test mass could be made of fused silica, with a radius of 10 cm and thickness of 16 cm. This aspect ratio is chosen to make equal the resonant frequencies of the two gravest internal modes (of the required symmetry). These will lie at $\omega_{1,2} = 2\pi \times 15.4$ kHz. Because the other modes fall at substantially higher frequencies, we can approximate the sum in Eq. (38) by its two lowest terms. If the loss factor appropriate to these resonances is a constant, 2.5×10^{-7} (Ref. 26), then the thermal noise is $x^2(\omega) = (1.4 \times 10^{-34} \text{ cm}^2/\text{Hz})(2\pi \text{ s}^{-1}/\omega)$.

The wires of this pendulum have their lowest transverse resonance at about 540 Hz. Below this frequency, the thermal noise from the wires is dominated by the contribution of this resonance. A calculation of the ratio of elastic energy to gravitational energy gives $\phi = \phi_w \times 10^{-4}$.

The net thermal noise from the wires is $x^2(\omega) = (6.7 \times 10^{-38} \text{ cm}^2/\text{Hz})(2\pi \text{ s}^{-1}/\omega)$.

As Fig. 6 shows, the fundamental mode of the pendulum is the dominant source of thermal noise at low frequencies. Above about 100 Hz, the strongest noise is the off-resonant thermal excitation of the lowest resonances of the test mass. The high- Q peaks from the wire resonances will also be visible. In a real gravitational-wave interferometer, seismic noise will probably dominate the noise budget at sufficiently low frequencies. Photon shot noise will be more important than thermal noise at the highest frequencies.³

ACKNOWLEDGMENTS

For stimulating discussions, I thank Alex Abramovici, David Bartlett, Peter Bender, Paul Boynton, David Cannel, Ron Drever, A. V. Granato, Joe Kovalik, Bob Krotkov, Peter Nelson, Riley Newman, Ho Jung Paik, Norna Robertson, Clive Speake, Bob Spero, Tuck Stebbins, Robbie Vogt, and Rai Weiss. This work was begun while the author was at the Department of Physics, Massachusetts Institute of Technology, and was supported in part by National Science Foundation Grant No. PHY-8803557. I thank the Joint Institute for Laboratory Astrophysics for financial support while this paper was being completed.

*Address starting January 1, 1991: Department of Physics, Syracuse University, Syracuse, NY 13244-1130.

¹R. V. Jones and C. W. McCombie, *Philos. Trans. R. Soc. A* **244**, 205 (1952).

²P. F. Michelson, J. C. Price, and R. C. Taber, *Science* **237**, 150 (1987), and references therein.

³R. Weiss, in *Sources of Gravitational Radiation*, edited by L. Smarr (Cambridge University Press, New York, 1979).

⁴P. G. Roll, R. Krotkov, and R. H. Dicke, *Ann. Phys. (N.Y.)* **26**, 442 (1964).

⁵C. C. Speake, *Proc. R. Soc. London A* **414**, 333 (1987); H. A. Chan and H. J. Paik, *Phys. Rev. D* **35**, 3551 (1987).

⁶M. C. Wang and G. E. Uhlenbeck, reprinted in *Selected Papers on Noise and Stochastic Processes*, edited by N. Wax (Dover, New York, 1954).

⁷H. B. Callen and R. F. Greene, *Phys. Rev.* **86**, 702 (1952); H. B. Callen and T. A. Welton, *ibid.* **83**, 34 (1951).

⁸C. W. Stubbs, Ph.D. thesis, University of Washington, 1988; P. Boynton, in *5th Force and Neutrino Physics*, proceedings of the Twenty-Third Rencontre de Moriond (Eighth Workshop), Les Arcs, France, 1988, edited by O. Fackler and J. Tran Thanh Van (Editions Frontières, Gif-sur-Yvette, France, 1988), pp. 431–44.

⁹H. J. Paik, Ph.D. thesis, Stanford University, 1974.

¹⁰V. B. Braginsky and A. B. Manukin, *Measurement of Weak Forces in Physics Experiments* (University of Chicago Press, Chicago, 1977).

¹¹V. B. Braginsky, V. P. Mitrofanov, and V. I. Panov, *Systems with Small Dissipation* (University of Chicago Press, Chicago, 1985).

¹²R. Weiss, P. S. Linsay, and P. R. Saulson, report, 1983 (unpublished).

¹³A. S. Nowick and B. S. Berry, *Anelastic Relaxation in Crystalline Solids* (Academic, New York, 1972).

¹⁴A. L. Kimball and D. E. Lovell, *Phys. Rev.* **30**, 948 (1927); W. P. Mason, in *Physical Acoustics: Principles and Methods*, edited by W. P. Mason and R. N. Thurston (Academic, New York, 1971), Vol. VIII, and references therein; C. C. Speake and T. J. Quinn, Report No. BIPM-87/3, 1987 (unpublished).

¹⁵L. D. Landau and E. M. Lifshitz, *Statistical Physics* (Pergamon, New York, 1980).

¹⁶J. L. Routbort and H. S. Sack, *J. Appl. Phys.* **37**, 4803 (1966).

¹⁷C. Zener, *Elasticity and Anelasticity of Metals* (University of Chicago Press, Chicago, 1948).

¹⁸H. W. Bode, *Network Analysis and Feedback Amplifier Design* (Krieger, Huntington, NY, 1975).

¹⁹C. Zener, *Phys. Rev.* **52**, 230 (1937); **53**, 90 (1938).

²⁰R. Weiss (private communication).

²¹L. Meirovitch, *Elements of Vibration Analysis* (McGraw-Hill, New York, 1975). The derivation below closely follows Meirovitch's treatment.

²²G. W. MacMahon, *J. Acoust. Soc. Am.* **36**, 85 (1964).

²³G. F. Franklin, J. D. Powell, and A. Emami-Naeini, *Feedback Control of Dynamic Systems* (Addison-Wesley, Reading, MA, 1986).

²⁴*American Institute of Physics Handbook*, 3rd ed., edited by D. E. Gray (McGraw-Hill, New York, 1972).

²⁵J. Kovalik and P. R. Saulson (unpublished).

²⁶Mitrofanov and Frontov (1974), cited by Braginsky, Mitrofanov, and Panov (Ref. 11).